Supplementary Information

Acetazolamide polymorphism: A case of hybridization induced polymorphism?

Sounak Sarkar, Mysore S. Pavan, Suryanarayan Cherukuvada and Tayur N. Guru Row*
Solid state and Structural Chemistry Unit,
Indian Institute of Science, Bangalore 560012, India

Contents

T-11: Topological features obtained for all covalent bonds in **II**

T-12: Atomic site coordinate systems

S-1: Experimental Section

Crystallization for Charge density study: Acetazolamide (AZM) was dissolved in boiling aqueous solution and single crystals of monoclinic form **II** ($P2_1/n$) were obtained upon slow cooling of the solution to room temperature. Good quality single crystals were chosen using a polarizing microscope and affixed to a Hampton Research Cryoloop using Paratone-N oil.

High temperature Crystallization Experiments: In a 100ml round bottom (rb) flask, 35 mg of AZM was dissolved in 20ml of in boiling water solution. Care was taken in maintaining the volume of the solution by putting a rubber septum in the neck of the rb flask. The temperature was ramped down in following ways:

1) The boiling solution was quenched in liquid nitrogen

2) The heating plate was switched off and hence the temperature was allowed to fall off under ambient condition-ambient cooling.

3) Controlled cooling to 30°C at a rate of 10°C/hr.

4) Controlled cooling to 30°C at a rate of 7°C/hr.

5) Controlled cooling to 30°C at a rate of 5°C/hr.

Data collection and structure refinement details

A crystal of dimensions 0.1 × 0.1 × 0.3 mm, was cooled to 100 K with a liquid nitrogen stream using an Oxford cobra open stream non-liquid nitrogen cooling device. X-ray diffraction data was collected on an Oxford Xcalibur (Mova) diffractometer equipped with an EOS CCD detector using MoKα radiation (λ= 0.71073 Å). The crystal to detector distance was fixed at 45 mm and the scan width (Δω) was 1° per frame during the data collection. The data collection strategy was chosen in such a way to yield a high resolution X-ray data set (d= 0.45 Å), with a high redundancy (7) and completeness of 100%. Cell refinement, data integration and reduction were carried out using the program CrysAlisPro.[1] Face indexing was done to facilitate accurate numerical absorption correction. Sorting, scaling, and merging of the data sets were carried out using the program SORTAV.[2] The crystal structure was solved by direct method using SHELXS2013and refined based on the spherical-atom approximation (based on F^2) using SHELXL2013[3] included in the WinGX package suite.[4] The hydrogen atom was located on the difference Fourier map and its position and isotropic thermal parameters were allowed to refine in the spherical atom model.

Multipole Modeling

The charge density modeling and multipolar aspherical atom refinements were performed based on the Hansen and Coppens multipole formalism using XD2015.[5] The function, $\Sigma w(|F_c|^2-K|F_o|^2)^2$ was minimized for all reflections with $I > 3\sigma(I)$. Weights (w) were taken as $1/\sigma^2 (F_o^2)$ and convergence criterion of the refinement was set to a maximal shift/esd $<10^{-10}$. Su-Clementi-Roetti wave functions[6] were used for the core and valence scattering factors of all the atoms. The resolution shells upto 1.11$\dot{A}^{-1}$ was divided into ten groups. Scale factors for each group were chosen (10 scale factors) and refined against the entire resolution range of diffraction data in the first refinement step.[7] The scatter plot of the variation of F_{obs} with F_{cal} is indicative of the quality of the data set after scaling (Fig.1). The positional and anisotropic displacement parameters of the non-hydrogen atoms were refined using reflection data with $\sin\theta/\lambda > 0.7$ $Å^{-1}$. In the next step of refinement, the position and displacement parameters of the non-hydrogen atoms were fixed to the refined values. The X—H bond lengths were constrained to the values reported by neutron diffraction experiments in literature.[8] The converged model was used to calculate anisotropic displacement parameters of H-atom using the SHADE2.1 server.[9] ADP value of the H-atom obtained from SHADE2.1 server was kept fixed during the subsequent multipole refinements.[10] Then the scale, positional and anisotropic displacement parameters, P_{val}, P_{lm}, and on non-hydrogen atoms were refined in a stepwise manner, until the convergence criterion was reached. κ and κ' were used to define for each non-hydrogen atom type based on chemical environment, while for the hydrogen atoms the value was fixed at 1.2. The multipole parameters of all the atoms in **II** were refined with no local symmetry and no chemical constraints. The multipole expansion was truncated upto hexadecapole level (l = 4) for only sulphur in **II**, where as for other non-hydrogen atoms it was truncated at the octupole level (l = 3) in both cases. For the H atoms, only monopole, bond directed dipole (d_z) and quadrupole (q_{3z^2-1}) components were refined during the multipole refinements. The multipole refinement was done keeping anisotropic harmonic model. The Hirshfeld rigid bond test[11] was applied to all covalent bonds involving non-hydrogen atoms to evaluate the quality of multipole modeling after the final cycle of refinement. The C(3)-C(4) single bond is found to have the largest difference of mean square displacement amplitude (DMSDA) value of 5×10^{-4}. The quantitative analysis of the electron density topology and related properties was performed using the XDPROP module of XD software suite.[12] Crystallographic refinement details of both spherical and multipolar model are summarized in Table 4. The hydrogen bonds in the structure have been summarized in Table 5.

Table 1. Resolution & Completeness Statistics (Cumulative and Friedel Pairs Averaged)

Theta	sin(th)/Lambda	Complete	Expected	Measured	Missing
20.82	0.500	0.999	841	840	1
23.01	0.550	0.999	1123	1122	1
25.24	0.600	0.999	1461	1460	1
					ACTA Min. Res. ---
27.51	0.650	0.999	1855	1854	1
29.84	0.700	1.000	2330	2329	1
32.21	0.750	1.000	2846	2845	1
34.65	0.800	1.000	3466	3465	1
37.17	0.850	1.000	4142	4141	1
39.77	0.900	1.000	4938	4937	1
42.47	0.950	1.000	5780	5779	1
45.29	1.000	1.000	6779	6778	1
48.27	1.050	1.000	7815	7814	1
51.43	1.100	1.000	9000	8999	1
52.08	1.110	1.000	9243	9242	1

Note: The Reported Completeness refers to the Actual H,K,L Index Range

Table 2. R-Value Statistics as a Function of Resolution (in Resolution Shell)

Theta	sin(Th)/L	#	R1	wR2	S	Rs	av(I/SigW)	av(I)	av(SigW)
12.38	0.302	183	0.054	0.152	2.483	0.026	15.83	1791.29	99.36
15.68	0.380	190	0.034	0.108	1.485	0.032	12.84	753.91	45.86
18.02	0.435	176	0.035	0.117	1.592	0.031	12.84	693.62	43.23
19.90	0.479	189	0.051	0.135	1.866	0.028	13.08	532.61	33.12
21.51	0.516	189	0.052	0.136	1.843	0.030	12.89	369.81	23.54
22.94	0.548	185	0.039	0.106	1.432	0.031	12.81	326.17	20.68
24.22	0.577	190	0.031	0.090	1.193	0.032	12.18	278.38	17.71
25.40	0.603	182	0.021	0.064	0.878	0.031	12.81	296.70	18.52
26.49	0.628	180	0.020	0.070	0.900	0.032	11.74	244.71	15.34
27.52	0.650	192	0.020	0.067	0.861	0.034	11.76	216.86	13.87
28.49	0.671	190	0.018	0.062	0.837	0.033	12.51	264.52	16.54
29.41	0.691	181	0.025	0.078	0.974	0.036	11.38	206.81	13.42
30.28	0.709	192	0.025	0.073	0.904	0.037	11.31	185.43	12.13
31.12	0.727	166	0.024	0.067	0.852	0.038	11.69	179.86	11.85
31.93	0.744	192	0.030	0.084	0.993	0.041	10.48	156.37	10.61
32.71	0.760	197	0.033	0.092	1.092	0.040	10.58	163.49	10.98
33.46	0.776	184	0.029	0.075	0.867	0.043	10.32	135.51	9.46
34.20	0.791	193	0.035	0.086	0.966	0.044	9.88	139.57	9.78
34.91	0.805	183	0.037	0.090	0.960	0.046	9.28	121.37	8.78
52.08	1.110	5708	0.042	0.110	0.872	0.080	6.41	54.74	5.60

R(sig) = sum(sig(I)) / sum(I) = 0.0409

From FCF: R1 = 0.0376(7485), wR2 = 0.1036(9242), S = 1.058
From CIF: R1 = 0.0376(7484), wR2 = 0.1035(9242), S = 1.058, Npar = 131

No (SHELXL) Optimized Weights: wR2 = 0.0883 , S = 1.54

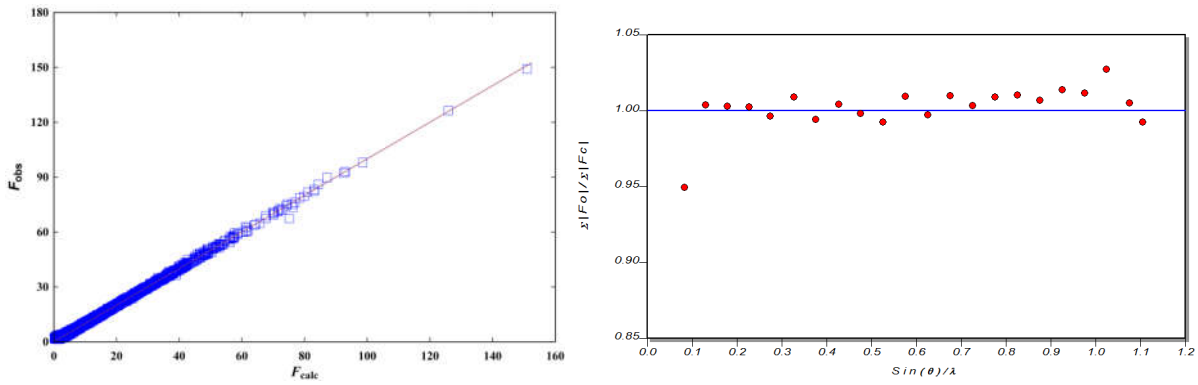

(a) (b)

Fig. 1 (a) Variation of F_{obs}/F_{cal} with $(\sin\theta)/\lambda$ (b) Scatter plot depicting the variation of F_{obs} with F_{cal} for **II**

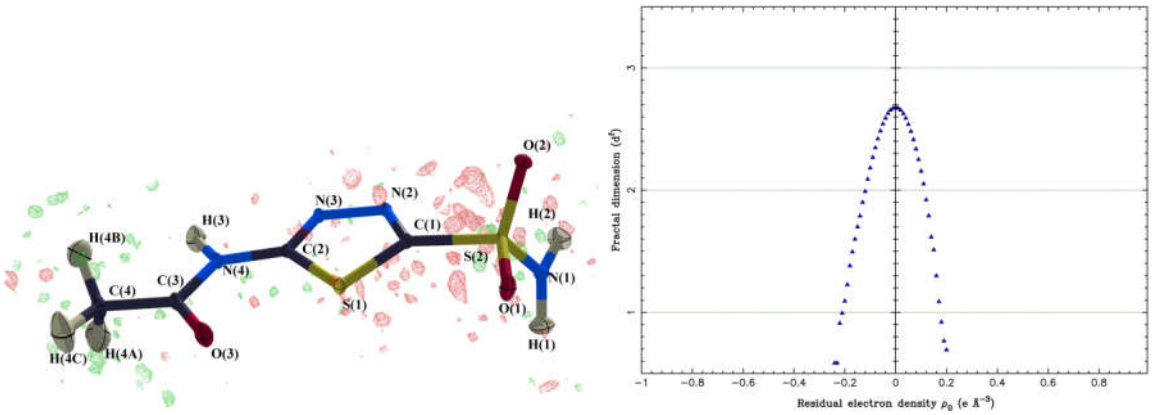

(a) (b)

Fig. 2 (a) 3D residual density plot at 0.2e $Å^{-3}$contour intervals (full resolution) (b) Fractal dimension plot for data ($\sin\theta/\lambda \leq 0.8 Å^{-1}$)

Computational details

Theoretical Charge Density

Positional parameters obtained from the experimental charge density model have been used for density functional calculations using the hybrid exchange correlational functional B3LYP[13, 14] with TZVP[15, 16] basis set included in CRYSTAL14[17] package. The shrinking factors

(IS1, IS2, and IS3) and the reciprocal lattice vectors were set to 3 (with 10 k-points in irreducible Brillouin zone). The bielectronic Coulomb and exchange series values for the truncation parameter were set as ITOL1_ITOL4 = 7 and ITOL5 = 14, respectively, for the calculations. The level shifter was set to 0.3 Hartree/cycle as 30% mixing of Fock/KS matrices (FMIXING) given in the input. An SCF convergence limit of the order of 10^{-6} Hartree was used. In the static model, atomic thermal displacement parameters for all atoms were set to zero. Structure factors were calculated for a resolution of 1.11$Å^{-1}$, which were used for the theoretical multipolar model. Refinements and analysis for the theoretical charge density model were performed using the XD software package following the same methodology used for the experimental charge density modeling.

NBO Calculation

The Natural Bond Orbital (NBO) method[18] has been used to analyze the stabilizing charge transfer from the lone pair orbital of nitrogen atom (LP) into the anti-bonding σ* orbital of S-C bond (BD*-S(2)-C(1)) of S-N bond. The NBO calculations are carried out in Gaussian09[19] at wB97XD[20] with a basis set of TZVP.[21] The inputs for the single point calculations are derived from the multipole model of **I**[22] and **II**. The outputs from the NBO calculation are viewed using Chemcraft 1.7.18.[23] Table 3 lists the details of the outcome from the NBO analysis of **I** and **II**. The conclusions can be made from the table-

1) LP of nitrogen atom in **II** is having pure p character while in case of **I**, LP of N atom is characterized by a mixture of s and p character.

2) Stabilization energy (second-order perturbation energies E(2)) corresponding to the intramolecular charge transfer in **II** is greater than **I**.

Table 3. NBO analysis of I and II

Polymorph	Type of orbital	Hybridization	Energy(a.u)	ΔE(a.u)	E(2) (kjmol^{-1})
II	LP-N(1)	s(0.32%) p99.99(99.67%)	-0.3946	0.5587	79.41
	BD*-S(2)-C(1)	s(20.99%) p3.69(77.50%)	0.16414		
I	LP-N(1)	s(12.95%) p6.72(87.01%)	-0.4424	0.6042	64.60
	BD*-S(2)-C(1)	s(20.86%) p 3.72(77.60%)	0.1617		

Geometry Optimization

For both form **I** and **II**, energy optimization (taking the initial geometry from crystalline phase minima) was performed using the integral equation formalism (IEF) version of the polarizable continuum solvation model (PCM)[24] at wb97xd/6-311++g(d,p) level (ref) to examine the dielectric field effect of crystallizing solvent (water) on the optimized conformation of AZM for both **I** and **II**.

There is a significant change in conformation of **II** from crystal geometry to the optimized geometry in solution (**IIA**). The prominent features observed are vast alteration in the S-N bond length, torsional angle τ(S-C-S-O), and dihedral angle Φ(S-N-H-H) indicated by the change of planar geometry to pyramidal geometry of NH_2 moiety (Fig. 3). On the other hand, the change in the conformation is minimal in case of transformation of **I** to **IA**.

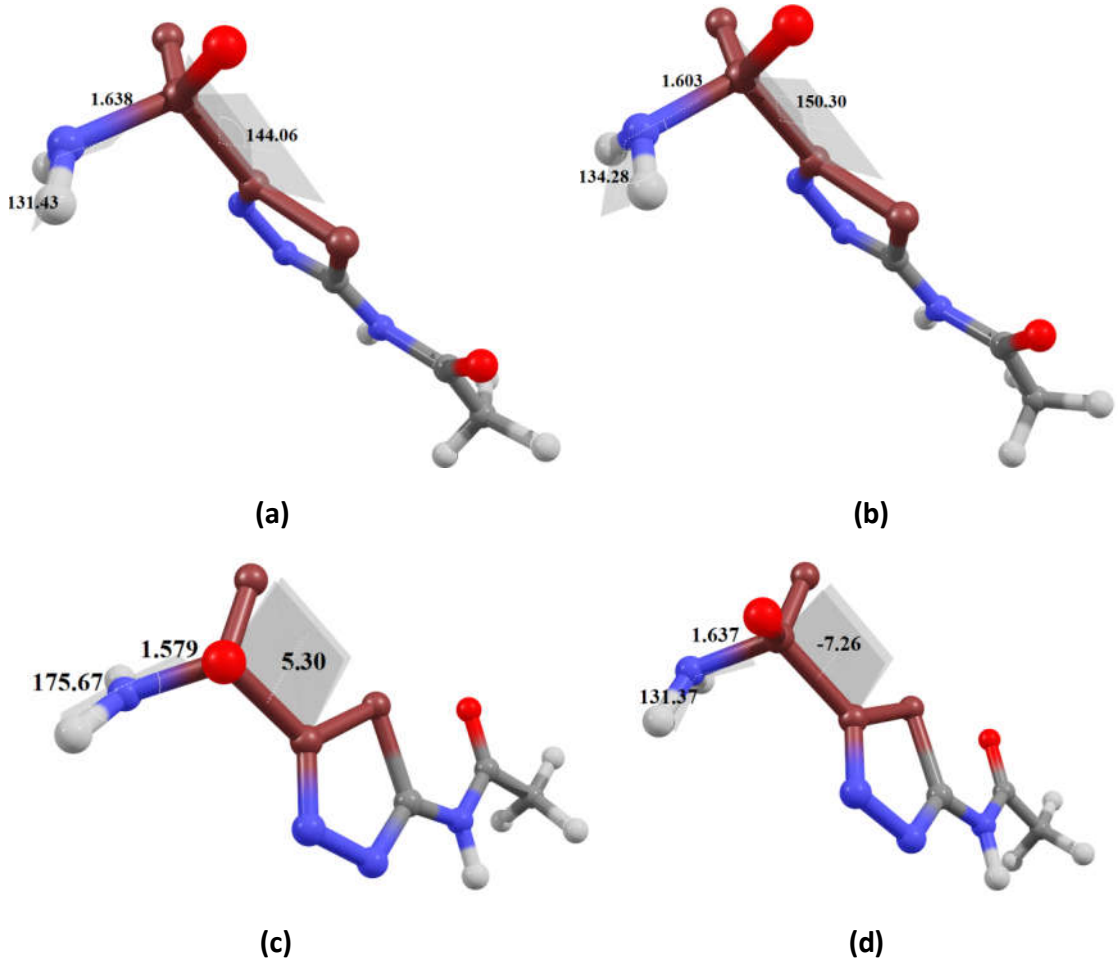

Fig. 3 (a) Molecular diagram of *P*-1 thermodynamic form (**I**)**. (b)** Molecular diagram of hydrated optimized conformations of **I** (**IA**). (**c**) Molecular diagram of $P2_1/n$ kinetic form. (**d**) Molecular

diagram of hydrated optimized conformations of **II** (**IIA**). τ (S-C-S-O) is coloured chocolate brown.

Potential Energy vs. Torsional angle τ (S-C-S-O) scan for AZM

Potential energy scan over the torsional angle τ (S-C-S-O) of AZM from 175° to -37.5° was performed at an interval of -2.5° in 85 steps. Calculation was performed in Polarizable Continuum Model (PCM)[19] at wb97xd/6-311++g(d,p) level

Potential Energy Scan For Dihedral angle Φ (S-N-H-H) scan for I and II

Dihedral angle was varied in case of **I** from 131.4° to 134.3° at an interval of 0.028515° in 100 steps. All calculation was performed in Polarizable Continuum Model (PCM)[19] at wb97xd/6-311++g(d,p) level. Dihedral angle was varied in case of **II** from 131.4° to 175.7° at an interval of 0. 0.443003 in 100 steps.

Table 4. Crystallographic table of the experimental structure

***CCDC* No.**	1451338	**$(\sin\theta/\lambda)_{max}$(Å^{-1})**	1.11
Mol. formula	$C_4H_6N_4O_3S_2$	**Reflns. collected**	65416
Formula weight	222.25	**Unique reflns.**	9242
Crystal system	Monoclinic	**Completeness (%)**	99.9
Space group	$P2_1/n$	**Redundancy**	7
a (Å)	4.7306(1)	**R_{int}**	0.053
b (Å)	21.6655(4)	***Spherical atom refinement***	
c (Å)	8.1069(1)	**R_1 (F)**	0.038
α (˚)	90	**wR_2 (F^2)**	0.103
β (˚)	103.803(2)	**Goodness-of-fit**	1.06
γ (˚)	90	**$\Delta\rho_{min,\ max}$ (eÅ^{-3})**	-0.52, 1.20
V (Å^3)	806.89(2)	**Multipole refinement**	
Z	4	**Reflns. used [I > 2σ(I)]**	7484
ρ_{calc} (g/cm^3)	1.830	**No of parameters**	392
F(000)	456	**R_1 (F^2)**	0.028
μ. (mm^{-1})	0.639	**wR_2 (F^2)**	0.051
T (K)	100(2)	**Goodness-of-fit**	0.9753
λ (Å)	0.71073	**$\Delta\rho_{min,\ max}$ (eÅ^{-3}) all data/ $\sin\theta/\lambda \leq 0.8$Å^{-1}**	-0.42, 0.32/ -0.24,0.20

Table 5. Hydrogen bonds observed in form **II**

Donor–H···Acceptor	D–H (Å)	H···A (Å)	D···A (Å)	∠D-H···A(°)	Symmetry Operator
N1–H1···N2	1.01	2.08	3.0120(6)	151	-1+x,y,z
N1–H1···O2	1.01	2.58	2.9298(8)	100	-1/2+x,1/2-y,1/2+z
N1–H2···O1	1.02	1.92	2.9300(7)	175	-1/2+x,1/2-y,1/2+z
N4–H3···N3	1.03	1.92	2.9474(6)	173	3-x,-y,1-z
C4–H4A···N1	1.08	2.59	3.5541(7)	148	2-x,-y,1-z

Powder X-ray diffraction and details of profile fitting

Powder X-ray diffraction data were collected on a Panalytical Empyrean powder diffractometer in reflection geometry using Cu as anode. Profile refinements (LeBail fit) were carried out using Jana2006.[25] Profile parameters such as GU, GV, GW, LX and LY are refined using Pseudo-Voigt function, in such a way that the profile fits best with the experimentally observed PXRD pattern. The values of cell parameters, (a,b,c, and symmetry unrestricted angles (for e.g., in case of monoclinic system only beta angle) of the two polymorphs are given as input which are further refined. This technique has been employed to examine the powder phases, as it is a superior way to check the phase purity than a simple peak matching. Any impurity, if present, will appear as a difference peak (Y_{obs}-Y_{calc}) indicative of the presence of a different phase.

The following representations are used in the powder X-ray diffractograms: - red dotted line: observed pattern, black line: fitted profile, blue line: difference curve between observed and calculated profiles (Y_{obs}-Y_{calc}), tick marks (red and blue): reflection positions of individual phases.

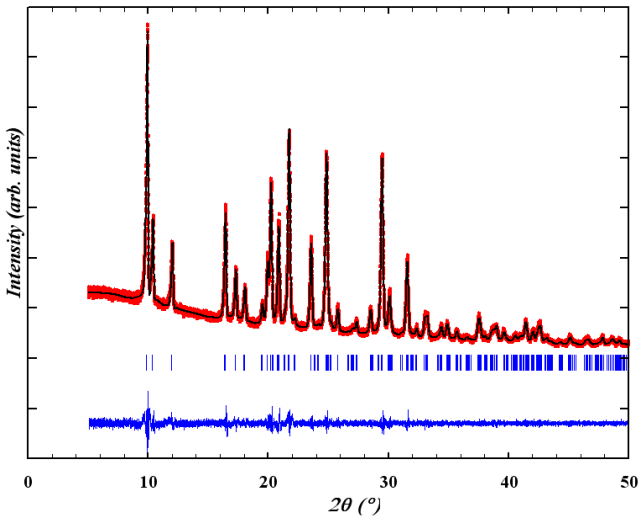

Fig. 4 Profile fitting of liquid nitrogen quenched sample

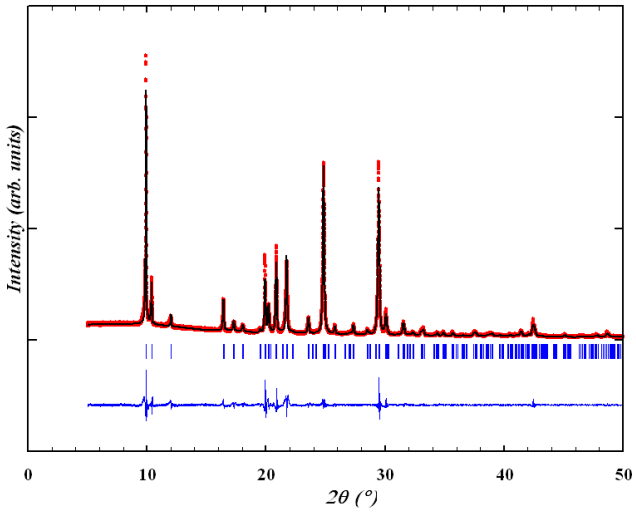

Fig. 5 Profile fitting of Ambient cooled sample

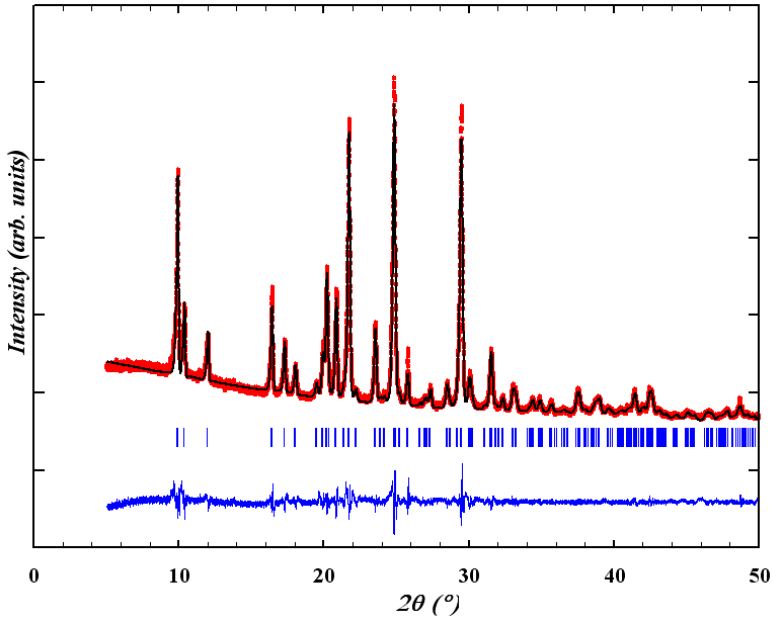

Fig. 6 Profile fitting of sample cooled at the rate of 10°C/hr

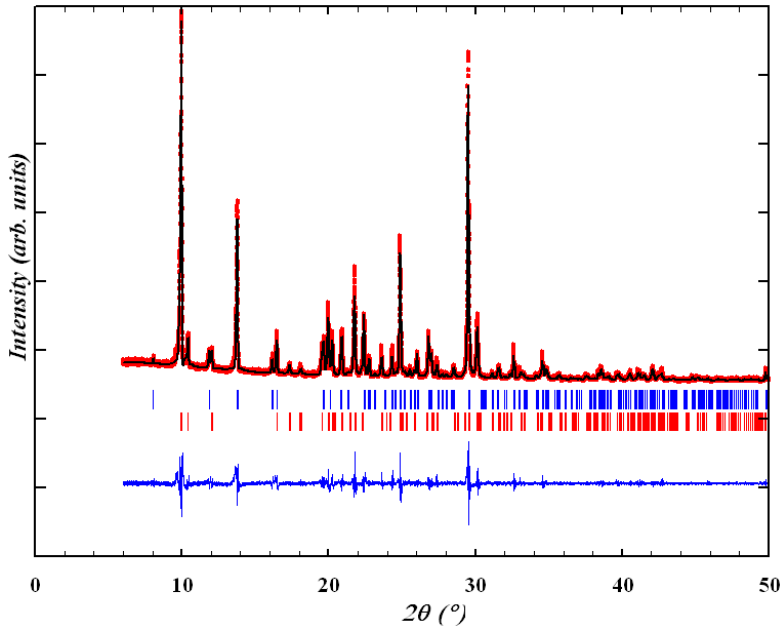

Fig. 7 Profile fitting of sample cooled at the rate of 7°C/hr

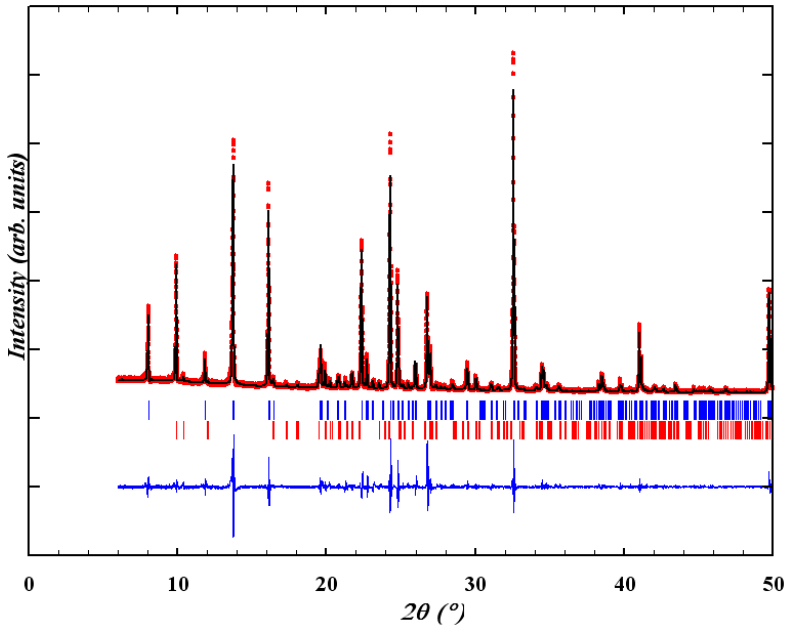

Fig. 8 Profile fitting of sample cooled at the rate of 5°C/hr

Table 6. Monopole Populations, Radial Parameters and Net Atomic Charges.

Atom	Pval	Kappa	P00	Kappa'	Atomic charge
S(1)	5.482	1.045	0	0.95	0.5182
S(2)	5.452	1.023	0	0.951	0.5479
O(1)	6.25	0.986	0	0.882	-0.2505
O(2)	6.331	0.986	0	0.882	-0.3309
O(3)	6.479	0.973	0	0.832	-0.4788
N(1)	5.183	0.991	0	0.971	-0.1832
N(2)	5.043	0.996	0	0.921	-0.0429
N(3)	5.083	0.996	0	0.921	-0.0828
N(4)	5.157	0.992	0	0.958	-0.1566
C(1)	4.119	1.008	0	0.984	-0.1188
C(2)	3.924	1.02	0	0.985	0.0764
C(3)	4.032	1.003	0	0.955	-0.0319
C(4)	5.164	0.952	0	0.968	-1.164
H(4A)	0.649	1.2	0	1.2	0.3509
H(4B)	0.654	1.2	0	1.2	0.3458
H(4C)	0.744	1.2	0	1.2	0.2561
H(1)	0.775	1.2	0	1.2	0.2246
H(3)	0.757	1.2	0	1.2	0.2426
H(2)	0.722	1.2	0	1.2	0.2782

Table 7. Dipole Population Parameters.

Atom	D11+	D11-	D10	Kappa'
S(1)	-0.043	-0.02	-0.034	0.95
S(2)	-0.068	0.004	0.069	0.951
O(1)	0.013	-0.033	-0.004	0.882
O(2)	0.064	0.001	-0.042	0.882
O(3)	-0.035	0.007	-0.061	0.832
N(1)	-0.007	0.033	0.005	0.971
N(2)	-0.019	-0.107	-0.036	0.921
N(3)	0.019	-0.125	-0.063	0.921
N(4)	0.013	-0.012	0.014	0.958
C(1)	0.031	0.041	0.028	0.984
C(2)	-0.006	-0.035	0.052	0.985
C(3)	-0.003	-0.019	0.064	0.955
C(4)	-0.153	0.026	0.046	0.968
H(4A)	0	0	0.073	1.2
H(4B)	0	0	0.034	1.2
H(4C)	0	0	0.08	1.2

H(1)	0	0	0.202	1.2
H(3)	0	0	0.176	1.2
H(2)	0	0	0.19	1.2

Table 8. Quadrupole Population Parameters.

Atom	Q20	Q21+	Q21-	Q22+	Q22-	Kappa'
S(1)	-0.112	0.057	0.148	0.102	-0.053	0.95
S(2)	0.108	0.116	-0.051	-0.071	0.086	0.951
O(1)	-0.028	-0.003	-0.027	-0.015	0.016	0.882
O(2)	-0.036	-0.003	0.008	-0.035	0.006	0.882
O(3)	0.032	-0.001	0.026	-0.104	0.01	0.832
N(1)	0.034	-0.01	-0.004	0.029	0.04	0.971
N(2)	0.078	-0.019	0.078	-0.073	0.001	0.921
N(3)	0.018	-0.019	0.108	-0.046	0.029	0.921
N(4)	0.027	0.005	0.016	0.02	-0.012	0.958
C(1)	0.138	0.018	0.032	-0.077	0.015	0.984
C(2)	0.148	-0.008	-0.004	-0.115	-0.006	0.985
C(3)	0.195	0.031	0.027	-0.167	0.007	0.955
C(4)	0.011	0.041	-0.032	-0.04	0.105	0.968
H(4A)	-0.097	0	0	0	0	1.2
H(4B)	-0.064	0	0	0	0	1.2
H(4C)	0.006	0	0	0	0	1.2
H(1)	0.111	0	0	0	0	1.2
H(3)	0.151	0	0	0	0	1.2
H(2)	0.052	0	0	0	0	1.2

Table 9. Octupole Population Parameters.

Atom	O30	O31+	O31-	O32+	O32-	O33+	O33-	Kappa'
S(1)	0.076	0.009	-0.101	0.026	0.004	0.004	-0.043	0.95
S(2)	0.421	-0.013	0.084	0.098	-0.068	0.059	-0.255	0.951
O(1)	0.016	0.005	-0.01	-0.013	-0.022	-0.019	0.028	0.882
O(2)	0.01	-0.017	-0.034	-0.018	0.005	0.006	0.013	0.882
O(3)	0.058	-0.002	-0.015	0.011	0.015	0.02	0.026	0.832
N(1)	0.141	-0.009	0.005	0.117	-0.004	0.016	-0.011	0.971
N(2)	0.144	0.02	-0.01	0.097	0.013	-0.001	-0.055	0.921
N(3)	0.072	0.008	-0.045	0.073	-0.002	-0.001	-0.049	0.921
N(4)	0.18	0.007	0.002	0.123	0.02	0.015	-0.036	0.958
C(1)	0.236	-0.03	-0.003	0.164	-0.033	0.015	0.005	0.984
C(2)	0.274	-0.02	0.012	0.216	0.035	-0.011	-0.011	0.985
C(3)	0.248	-0.03	-0.048	0.231	0.001	-0.016	-0.012	0.955
C(4)	0.231	0.018	0.007	0.008	0.143	0.003	-0.233	0.968

Table 10. Hexadecapole Population Parameters.

Atom	H40	H41+	H41-	H42+	H42-	H43+	H43-	H44+	H44-	Kappa'
S(1)	0.06	-0.019	-0.049	0.032	0.024	0.032	-0.05	0.032	-0.035	0.95
S(2)	0.017	-0.057	-0.004	-0.021	-0.009	-0.04	0.172	-0.018	-0.004	0.951
O(1)	0	0	0	0	0	0	0	0	0	0.882
O(2)	0	0	0	0	0	0	0	0	0	0.882
O(3)	0	0	0	0	0	0	0	0	0	0.832
N(1)	0	0	0	0	0	0	0	0	0	0.971
N(2)	0	0	0	0	0	0	0	0	0	0.921
N(3)	0	0	0	0	0	0	0	0	0	0.921
N(4)	0	0	0	0	0	0	0	0	0	0.958
C(1)	0	0	0	0	0	0	0	0	0	0.984
C(2)	0	0	0	0	0	0	0	0	0	0.985
C(3)	0	0	0	0	0	0	0	0	0	0.955
C(4)	0	0	0	0	0	0	0	0	0	0.968

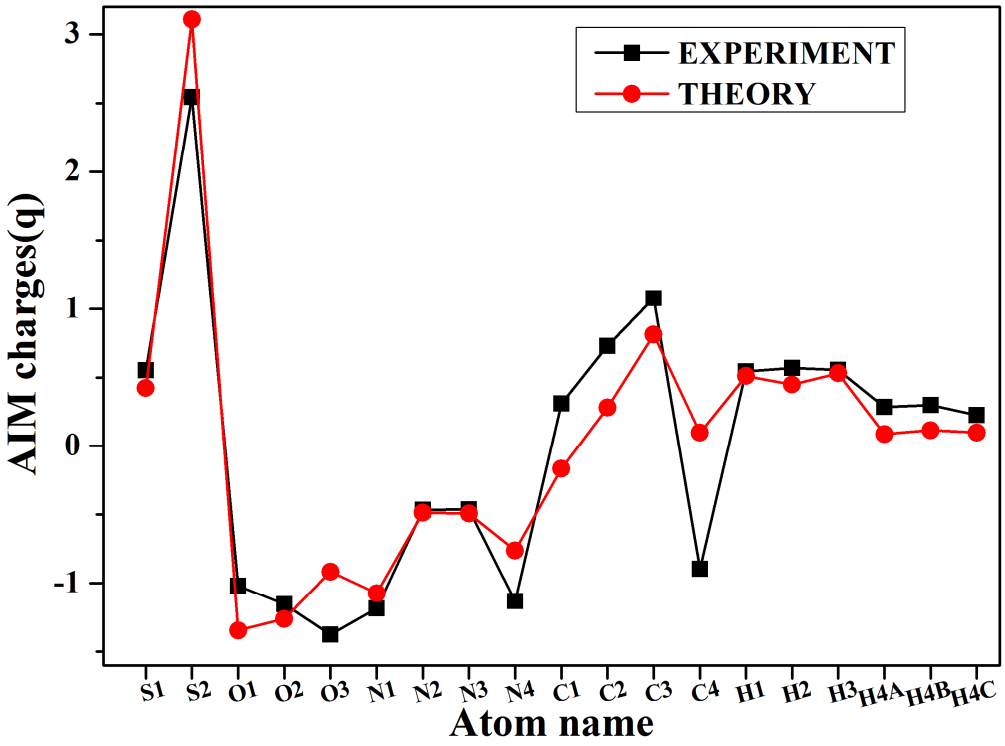

Fig. 9 Comparison between experiment and theory AIM charges

Table 11. Topological features obtained for all covalent bonds in **II.** r_1 and r_2 are the distances from the BCP to the first atom (A) and second atom (B), respectively. The interaction length, R_{ij} = (r1 + r2). The values obtained from periodic calculations using the B3LYP/TZVP method are given in italics.

Atom A	Atom B	R_{ij}(Å) (A-B)	r_1(Å) (A-CP)	r_2(Å) (CP-B)	$\rho(r)_{cp}$ (eÅ^{-3})	$\nabla^2\rho$ (eÅ^{-5})	λ_1	λ_2	λ_3	ε
O(3)	S(1)	2.6075	1.2735	1.334	0.16	2.19	-0.49	-0.47	3.15	0.04
		2.6058	*1.2206*	*1.3852*	*0.2*	*2.45*	*-0.63*	*-0.56*	*3.64*	*0.11*
C(1)	S(1)	1.7303	0.8519	0.8784	1.27	-3.61	-7.92	-5.92	10.23	0.34
		1.7319	*0.7754*	*0.9565*	*1.39*	*-7.38*	*-7.13*	*-5.22*	*4.96*	*0.37*
C(2)	S(1)	1.7294	0.8416	0.8878	1.38	-5.57	-9.25	-7	10.68	0.32
		1.7299	*0.802*	*0.9279*	*1.38*	*-6.93*	*-6.89*	*-5.86*	*5.83*	*0.18*
S(2)	O(1)	1.4415	0.6226	0.8189	2.39	-17.85	-19.34	-18.96	20.45	0.02
		1.4418	*0.5855*	*0.8563*	*1.9*	*17.96*	*-10.87*	*-10.18*	*39.01*	*0.07*
S(2)	O(2)	1.4312	0.6191	0.8121	2.39	-11.79	-17.38	-16.18	21.76	0.07
		1.4316	*0.5827*	*0.8489*	*1.97*	*15.81*	*-12.69*	*-12.01*	*40.51*	*0.06*
S(2)	N(1)	1.5791	0.7851	0.794	2.1	-19.76	-16.94	-15.78	12.96	0.16
		1.5799	*0.6407*	*0.9392*	*1.64*	*-6.34*	*-9.41*	*-8.06*	*11.13*	*0.17*
C(1)	S(2)	1.7777	0.8572	0.9205	1.28	-5.33	-8.27	-7.16	10.1	0.15
		1.7779	*0.8142*	*0.9637*	*1.33*	*-8.26*	*-6.98*	*-6.33*	*5.05*	*0.1*
C(3)	O(3)	1.2229	0.4257	0.7972	2.96	-27.1	-29.1	-25.22	27.22	0.15
		1.2229	*0.486*	*0.7369*	*2.93*	*-33.85*	*-26.3*	*-23.18*	*15.62*	*0.13*
H(1)	N(1)	1.0154	0.2599	0.7555	2.28	-35.61	-32.09	-30.29	26.76	0.06
		1.0154	*0.2849*	*0.7305*	*2.28*	*-34.22*	*-31.05*	*-29.14*	*25.97*	*0.07*
H(2)	N(1)	1.0157	0.2568	0.7589	2.14	-30.91	-29.18	-27.97	26.25	0.04
		1.0156	*0.2991*	*0.7165*	*2.31*	*-34.35*	*-30.97*	*-28.52*	*25.14*	*0.09*
N(3)	N(2)	1.3709	0.6795	0.6914	2.19	-1.33	-16.55	-16.41	31.63	0.01
		1.3711	*0.6779*	*0.6932*	*2.04*	*6.08*	*-14.48*	*-14.2*	*34.76*	*0.02*
C(1)	N(2)	1.3013	0.544	0.7573	2.64	-30.2	-23.64	-19.07	12.51	0.24
		1.3012	*0.5759*	*0.7253*	*2.61*	*-23.95*	*-21.35*	*-17.82*	*15.22*	*0.2*
C(2)	N(3)	1.3221	0.6042	0.7179	2.47	-21.03	-21.66	-17.17	17.8	0.26
		1.322	*0.6082*	*0.7138*	*2.47*	*-18.05*	*-19.68*	*-16.7*	*18.33*	*0.18*
C(2)	N(4)	1.3651	0.5797	0.7854	2.26	-22.57	-20.22	-16.28	13.93	0.24
		1.3653	*0.6314*	*0.7339*	*2.23*	*-15.3*	*-18.26*	*-15.43*	*18.38*	*0.18*
C(3)	N(4)	1.3836	0.5878	0.7958	2.19	-19.39	-18.05	-15.06	13.71	0.2
		1.3834	*0.6228*	*0.7606*	*2.09*	*-13.39*	*-16.94*	*-14.34*	*17.88*	*0.18*
H(3)	N(4)	1.0299	0.2565	0.7734	2.22	-36.65	-32.11	-30.46	25.92	0.05
		1.03	*0.2856*	*0.7444*	*2.15*	*-26.11*	*-28.46*	*-26.83*	*29.18*	*0.06*
C(4)	C(3)	1.4948	0.6962	0.7986	1.82	-15.33	-13.02	-11.34	9.03	0.15
		1.4942	*0.6934*	*0.8008*	*1.76*	*-10.19*	*-12.19*	*-11.48*	*13.48*	*0.06*
H(4A)	C(4)	1.0772	0.3145	0.7627	1.61	-10.06	-15.12	-13	18.06	0.16
		1.0771	*0.4201*	*0.657*	*1.96*	*-18.99*	*-17.82*	*-17.25*	*16.08*	*0.03*
H(4B)	C(4)	1.0802	0.2993	0.7809	1.61	-9.61	-15.2	-14.21	19.81	0.07
		1.0793	*0.4169*	*0.6624*	*1.93*	*-17.74*	*-17.11*	*-16.93*	*16.3*	*0.01*
H(4C)	C(4)	1.0764	0.325	0.7514	1.82	-17.13	-18.23	-16.54	17.63	0.1
		1.0764	*0.4071*	*0.6693*	*1.98*	*-19.68*	*-18.29*	*-17.93*	*16.54*	*0.02*

Table 12. Atomic site coordinate systems

ATOM	ATOMS			V1	DISTANCE	ATOMS			V2	DISTANCE	R/L
S(1)	S(1)	-	C(1)	Z	1.729	S(1)	-	C(2)	Y	1.729	R
S(2)	S(2)	-	O(2)	Z	1.431	S(2)	-	O(1)	Y	1.441	R
O(1)	O(1)	-	S(2)	Z	1.441	O(1)	-	N(1)	Y	2.469	R
O(2)	O(2)	-	S(2)	Z	1.431	O(2)	-	N(1)	Y	2.44	R
O(3)	O(3)	-	C(3)	Z	1.223	O(3)	-	N(4)	Y	2.262	R
N(1)	N(1)	-	H(1)	Z	1.015	N(1)	-	H(2)	Y	1.016	R
N(2)	N(2)	-	C(1)	Z	1.301	N(2)	-	N(3)	Y	1.371	R
N(3)	N(3)	-	C(2)	Z	1.322	N(3)	-	N(2)	Y	1.371	R
N(4)	N(4)	-	H(3)	Z	1.03	N(4)	-	C(2)	Y	1.365	R
C(1)	C(1)	-	N(2)	Z	1.301	C(1)	-	S(1)	Y	1.729	R
C(2)	C(2)	-	N(3)	Z	1.322	C(2)	-	N(4)	Y	1.365	R
C(3)	C(3)	-	O(3)	Z	1.223	C(3)	-	N(4)	Y	1.383	R
C(4)	C(4)	-	H(4A)	Z	1.077	C(4)	-	H(4C)	Y	1.076	R
H(4A)	H(4A)	-	C(4)	Z	1.077	H(4A)	-	H(4C)	Y	1.759	R
H(4B)	H(4B)	-	C(4)	Z	1.079	H(4B)	-	H(4C)	Y	1.758	R
H(4C)	H(4C)	-	C(4)	Z	1.076	H(4C)	-	H(4A)	Y	1.759	R
H(1)	H(1)	-	N(1)	Z	1.015	H(1)	-	H(2)	Y	1.827	R
H(3)	H(3)	-	N(4)	Z	1.03	H(3)	-	C(2)	Y	2.063	R
H(2)	H(2)	-	N(1)	Z	1.016	H(2)	-	H(1)	Y	1.827	R

References:

1. M. Mathew and G. J. Palenik, *Chem. Soc. Perkin Trans*, 1974, 532-536.
2. R. H. Blessing, *J. Appl. Crystallogr.*, 1997, **30**, 421-426.
3. GM. Sheldrick, *SHELXS-2013,Program for structure solution*, 2013
4. L. J. Farrugia, *J. Appl. Crystallogr.*, 2012, **45**, 849-854.
5. T. Koritsanszky, P. Mallinson, P. Macchi, A. Volkov, C. Gatti, C.-I. Milano, T. Richter and L. Farrugia, *XD2015 - a computer program for multipole refinement, topological analysis of charge densities and evaluation of intermolecular energies from experimental or theoretical structure factors*, 2015.
6. E. Clementi and C. Roetti, *At. Data Nucl. Data Tables*, 1974, **14**, 177-478.
7. B. Niepotter, R. Herbst-Irmer and D. Stalke, *J. Appl. Cryst*, 2015, **48**, 1485-1497.
8. F. H. Allen and I. J. Bruno, *Acta Crystallogr. Sect. B: Struct. Sci.*, 2010, **66**, 380-386.
9. A. O. Madsen, *J. Appl. Crystallogr.*, 2006, **39**, 757-758.
10. N. K. Hansen and P. Coppens, *Acta Crystallographica Section A: Crystal Physics, Diffraction, Theoretical and General Crystallography*, 1978, **34**, 909-921.
11. F. Hirshfeld, *Acta Crystallographica Section A: Crystal Physics, Diffraction, Theoretical and General Crystallography*, 1976, **32**, 239-244.

12. A. Volkov, Y. Abramov, P. Coppens and C. Gatti, *Acta Crystallogr. Sect. A: Found. Crystallogr.*, 2000, **56**, 332-339.
13. C. Lee, W. Yang and R. G. Parr, *Phys. Rev. B*, 1988, **37**, 785.
14. A. D. Becke, *J. Chem. Phys.*, 1996, **104**, 1040-1046.
15. A. Schäfer, H. Horn and R. Ahlrichs, *The Journal of Chemical Physics*, 1992, **97**, 2571-2577.
16. M. F. Peintinger, D. V. Oliveira and T. Bredow, *J. Comput. Chem.*, 2013, **34**, 451-459.
17. R. Dovesi, V. Saunders, C. Roetti, R. Orlando, C. Zicovich-Wilson, F. Pascale, B. Civalleri, K. Doll, N. Harrison and I. Bush, *Università di Torino, Torino*, 2013.
18. A. E. Reed, L. A. Curtiss and F. Weinhold, *Chem. Rev.*, 1988, **88**, 899-926.
19. M. Frisch, G. Trucks, H. B. Schlegel, G. Scuseria, M. Robb, J. Cheeseman, G. Scalmani, V. Barone, B. Mennucci and G. Petersson, *Inc., Wallingford, CT*, 2009, **200**.
20. J.-D. Chai, 2009.
21. A. Schäfer, C. Huber and R. Ahlrichs, *J.Chem.Phys.*, 1994, **100**, 5829-5835.
22. S. P. Thomas, D. Jayatilaka and T. N. Guru Row, *Phys. Chem. Chem. Phys.*, 2015, **17**, 25411-25420.
23. G. Zhurko, *Chemcraft, Version 1.7 (build 365)*.
24. J. Tomasi, B. Mennucci and R. Cammi, *Chem. Rev.*, 2005, **105**, 2999-3094.
25. V. PetríCek, M. Dusek and L. Palatinus, *Z. Kristallogr*, **229**, 345-352.